Received: 23 September 2024 | Revised: 26 November 2024 | Accepted: 16 December 2024

DOI: 10.1096/fj.202402278RR

RESEARCH ARTICLE

The FASEB Journal

The C3/C3aR pathway exacerbates acetaminophen-induced mouse liver injury via upregulating podoplanin on the macrophage

Zhanli Xie[1,2] | **Jiang Jiang**[3] | **Fei Yang**[1] | **Jingjing Han**[1] | **Zhenni Ma**[1] | **Tao Wen**[4] | **Xia Bai**[1,5,6]

[1]Jiangsu Institute of Hematology, National Clinical Research Center for Hematologic Diseases, NHC Key Laboratory of Thrombosis and Hemostasis, The First Affiliated Hospital of Soochow University, Suzhou, China

[2]Institute of Clinical Medicine Research, Suzhou Hospital, Affiliated Hospital of Medical School, Nanjing University, Suzhou, China

[3]Department of Nuclear Medicine, The Second Affiliated Hospital of Soochow University, Suzhou, China

[4]Medical Research Center, Beijing Chao-Yang Hospital, Capital Medical University, Beijing, China

[5]Institute of Blood and Marrow Transplantation, Collaborative Innovation Center of Hematology, Soochow University, Suzhou, China

[6]State Key Laboratory of Radiation Medicine and Protection, Soochow University, Suzhou, China

Correspondence
Tao Wen, Medical Research Center, Beijing Chao-Yang Hospital, Capital Medical University, Gongti South Rd, Chao-Yang District, Beijing 100020, China.
Email: wentao5281@163.com

Xia Bai, Jiangsu Institute of Hematology, National Clinical Research Center for Hematologic Diseases, NHC Key Laboratory of Thrombosis and Hemostasis, The First Affiliated Hospital of Soochow University, 188 Shizi Street, Suzhou 215006, China.
Email: baixia@suda.edu.cn

Funding information
Suzhou People's Livelihood Science and Technology Project, Grant/Award Number: SKY2022155 and SKJYD2021089; Priority Academic Program Development of Jiangsu Higher Education Institutions

Abstract

Acute liver failure (ALF) is a life-threatening condition that occurs when the liver sustains severe damage and rapidly loses its function. The primary cause of ALF is the overdose of acetaminophen (APAP), and its treatment is relatively limited. The involvement of the complement system in the development of ALF has been implicated. However, the related mechanisms remain poorly understood. Complement 3 (*C3*) knockout mice, complement 3a receptor (C3aR) knockout mice, platelet C-type lectin-like receptor 2 (*Clec-2*)–deficient mice, and myeloid cell podoplanin (*Pdpn*)-deficient mice were generated. Liver tissues were collected for histological analysis, RNA sequencing, confocal immunofluorescence, and immunoblot analyses. Our data demonstrated that APAP activated the C3/C3aR pathway, leading to intrahepatic hemorrhage, ultimately resulting in hepatocyte necrosis. Deletion of C3 or C3aR mitigated APAP-induced liver injury (AILI). C3/C3aR signaling upregulated the expression and phosphorylation of transcription factors STAT3 and c-Fos in hepatic Kupffer cells, which in turn increased PDPN expression, promoting platelet recruitment to the Kupffer cells via the interaction of PDPN and the CLEC-2 on platelets. Since the activation of platelets mediated

Abbreviations: AILI, APAP-induced liver injury; ALF, acute liver failure; ALT, alanine transferase; APAP, acetaminophen; AST, aspartate aminotransferase; C3, complement 3; C3aR, complement 3a receptor; CLEC-2, C-type lectin-like receptor 2; EGFR, epidermal growth factor receptor; ELISA, enzyme-linked immunosorbent assay; H&E, hematoxylin and eosin stain; LDH, lactate dehydrogenase; LysM *Pdpn*$^{-/-}$, myeloid cell PDPN-deficient mice; MAC, membrane attack complex; OCT, optimum cutting temperature compound; PDPN, podoplanin; Plt *Clec-2*$^{-/-}$, specific deletion of platelet CLEC-2; rmC3, recombinant mouse C3 protein; RT-PCR, real-time quantitative PCR; SDS-PAGE, Polyacrylamide gel electrophoresis.

Zhanli Xie and Jiang Jiang contributed equally to this work.

by C3/C3aR occurs irrespective of the major hemostatic pathways, blocking the C3/C3aR pathway in ALF could be a coagulopathy-sparing and novel therapeutic approach. In summary, this study unveiled the critical roles of the C3/C3aR pathway in developing AILI, providing evidence that the C3/C3aR pathway could be an effective therapeutic target for AILI.

KEYWORDS

C3/C3aR pathway, CLEC-2, Kupffer cell, liver injury, PDPN

1 | INTRODUCTION

Acute liver failure (ALF) is a life-threatening condition characterized by severe damage and dysfunction of liver cells, often leading to multiple organ failure or even death.[1] Acetaminophen (APAP), also known as paracetamol or N-acetyl-p-aminophenol, is among the most widely used drugs globally.[2] At therapeutic doses, it is an effective analgesic and antipyretic medication generally well-tolerated by both children and adults. The leading cause of ALF worldwide is hepatotoxicity, with APAP overdose serving as a prime example.[3] Despite the clinical significance of APAP-induced hepatotoxicity, only one antidote, N-acetylcysteine, has gained approval for clinical use.[4,5] Consequently, the need for a specific and effective therapy to reverse or alleviate APAP-related acute liver injury (ALI) remains unmet. The difference between female and male mice in AILI has been well confirmed.[6] The liver necrosis in female mice is usually less than in male mice, regardless of their genetic background. Therefore, most studies only use female or male mice to obtain comparable results. In our study, male mice were only used.

The liver injury induced by excessive APAP in human ALF follows a specific pattern, and the biochemical signs of liver injury become evident within 24–48 h.[7] APAP stimulates the body to produce various proinflammatory mediators, including chemokines, cytokines, and reactive oxygen species or nitrogen species, which induce necrotic changes in liver cells.[8,9] The direct toxicity of APAP can trigger inflammatory and coagulation cascade, leading to the progression and deterioration of acetaminophen-induced liver injury (AILI).[10] Although usually not cause obvious bleeding symptoms, significant changes in the hemostatic system, such as decreased platelet count, are observed in mice with APAP-induced liver failure.[11,12] Severe thrombocytopenia is correlated with poor prognosis during the onset of ALI.[13] Reports indicate that APAP-induced thrombocytopenia is linked to platelet accumulation in the liver in mice, and the absence of platelet aggregates dramatically accelerates the repair of the injured liver.[11] These findings suggest that platelet recruitment with the liver is an important mechanism contributing to AILI. However, limited knowledge exists regarding the potential platelet aggregation mechanism in AILI. Furthermore, it remains uncertain whether attenuating platelet aggregation could mitigate AILI.

The complement system plays a vital role in liver homeostasis and immune response, participating in the pathogenesis of multiple diseases.[14] All three pathways, namely the classical pathway, the alternative pathway, and the lectin pathway, ultimately lead to the activation of the central component Complement 3 (C3). The liver is the primary site for complement synthesis.[14] In mice, C3 deficiency protects against liver ischemia–reperfusion injury.[15] The complement system enhances the tolerance of fatty liver to ischemia–reperfusion injury.[16] During ALI, the complement system activation is triggered by pathogens,[17] and the controlled activation of complements is beneficial for clearing pathogens.[18] However, excessive complement system activation can lead to organ damage.[19] Therefore, inhibition of complement activation might help protect liver function in AILI.

Nevertheless, it remains to be seen how complement activation is autonomously controlled within AILI. Our prior research has demonstrated the key role of the complement in promoting platelet accumulation in sepsis-induced liver injury.[20] Determination of Thrombin-antithrombin complex (TAT) plasma levels in wild-type and $C3^{-/-}$ mice by ELISA.[21] Considering the pivotal role of intrahepatic coagulation in AILI's pathogenesis, we wanted to investigate whether the complement system contributes to the accumulation of platelets in the liver during the AILI process.

This study aimed to investigate the role of C3 in AILI, and we demonstrated elevated C3 levels in mice challenged with APAP overdose. Our data revealed a central role of the C3/Complement 3a receptor (C3aR) pathway in the hepatic platelet recruitment via podoplanin (PDPN)/C-type lectin-like receptor 2 (CLEC-2) during AILI. Therefore, we hypothesize that targeted regulation of the C3/C3aR pathway is a promising early interventional strategy for ALF.

2 | MATERIALS AND METHODS

2.1 | Reagents

APAP (M3301) was purchased from AbMole (Houston, USA). Mouse C3 protein (AP76294) was purchased from SAB (MD, USA). ELISA kits for IL-1β (EK0502), TNF-α (EK1352), and IL-6 (EK1222) were purchased from SAB (MD, USA). Rabbit monoclonal P-selectin antibody (60322), rabbit polyclonal anti-STAT3 antibody (21045), anti-p-STAT3 antibody (11045), c-Fos antibody (40731), and p-c-Fos antibody (12257) were purchased from SAB. Rabbit monoclonal anti-C3 antibody (ab97462), rat monoclonal anti-F4/80 antibody (ab6640), rabbit polyclonal anti-TNF-α antibody (ab6671), rabbit polyclonal anti-IL-1β antibody (ab179570), rabbit polyclonal anti-C5b-9 antibody (ab55811), Syrian hamster monoclonal anti-PDPN antibody (ab92319), rabbit monoclonal anti-CD41 antibody (ab134131), rabbit monoclonal Fibronectin antibody (ab268020), rabbit monoclonal anti-C3aR antibody (ab288413), chicken polyclonal anti-albumin antibody (ab106582), rabbit polyclonal anti-glyceraldehyde-3-phosphate dehydrogenase (GAPDH) antibody (AB0037), Alexa Fluor 405–conjugated goat anti-chicken IgG antibody (ab175674), Alexa Fluor 594–conjugated goat anti-rat IgG (ab150160), and Alexa Fluor 647–conjugated donkey anti-rabbit IgG antibody (ab150075) were purchased from Abcam. Goat anti-rabbit IgG secondary antibody HRP conjugated (#L35017) was purchased from SAB (MD, USA). LDH assay kit (ab102526) was purchased from Abcam. ApopTag fluorescein in situ apoptosis detection kit (S7110) was purchased from Millipore (Boston, USA). Thrombin was purchased from Chrono-Log (Havertown, USA).

2.2 | Animal experiments

C3$^{-/-}$ mice (Stock No: 029661) were purchased from The Jackson Laboratory, while *C3aR*$^{-/-}$ mice (KOCMP-12267-C3ar1-B6J-VA) were purchased from the Cyagen Co. Pf4-Cre mice, LysM-Cre mice and C57BL/6J (B6, CD45.2) were also obtained from The Jackson Laboratory. Platelet CLEC-2–deficient mice (Plt *Clec2*$^{-/-}$) were generated by crossing *Clec-2*$^{fl/fl}$ mice with Pf4-Cre mice. Myeloid cell PDPN-deficient mice (LysM *Pdpn*$^{-/-}$) were generated by crossing *Pdpn*$^{fl/fl}$ mice with LysM-Cre mice.[20] For APAP treatment, mice and their littermates were controlled at 8 weeks old and intraperitoneally injected with 350 mg/kg of the reagent.[22] Male mice were predominantly used in ALI studies as reported in the literature.[23] Therefore, male mice were employed for most of the experiments in this study. In some experiments, mice treated with APAP were immediately intraperitoneally injected with physiological saline (100 mL) or recombinant mouse C3 protein (500 ng/ mouse). At the time points indicated in the legend, livers were collected, and frozen sections were used for immunofluorescence (IF) staining to detect MFs and platelets using anti-F4/80 and anti-CD41 antibodies, respectively. Liver paraffin sections were made, and serum was collected for H&E staining and biomarker assays to detect liver injury. All animal experiments were approved by the Institutional Animal Care and Use Committee (IACUC) of Soochow University (IRB202003006RI, March 20, 2020) and were performed in accordance with the guidelines of Soochow University for animal experiments.

2.3 | Complement hemolytic test

The complement hemolytic activity of mouse sera was measured using standard methods and reported based on its ability to dissolve chicken erythrocytes pre-sensitized with erythrocyte-specific antibodies.[24] The detailed steps are as follows: (1) Dilute normal B10D2nSn Slc mouse serum to a 1:10 ratio in gelatin-buffered physiological saline (GVBS) (B100, CompTech, Tyler, TX) as a 100% dissolution control. (2) Dilute the experimental samples to a 1:10 ratio in GVBS and mixed them with human C5-deficient serum and GVBS. Repeat each sample three times; (3) Add two μL of 500 mmol/L EDTA to the third well as a "hemolysis free" color control standard; (4) Pre-sensitize chicken red blood cells with anti-chicken red blood cell polyclonal antibodies at 4°C for 15 min; (5) Add the pre-sensitized chicken red blood cells to the plate and incubate at 37°C for 30 min; (6) After centrifugation, transfer the supernatant to a microplate titration plate; (7) Use a microplate reader to measure the absorbance at OD415; (8) Calculate the degree of hemolysis using the following formula:% hemolysis = 100 × (OD sample − OD sample chromaticity control)/(OD 100% dissolution control − OD 100% dissolution chromaticity control).

2.4 | Reverse transcription-quantitative real-time PCR (RT-qPCR)

Total RNA was isolated from mouse livers using TRIzol, and the RNA (2 μg) was used for reverse transcription. The RT-qPCR was performed using SYBR Green Master Mix in 20 μL reaction volumes. The samples were analyzed in duplicates, with GAPDH as the internal control. The RT-qPCR primer sequences are listed in Table S1.

2.5 | Immunofluorescence analysis

Mouse livers were collected and fixed with 4% formalin. After overnight dehydration with 20% sucrose at 4°C, the livers were embedded in an OCT complex (Tissue Tek, Sakura Finetek). Frozen sections of 15 μm thickness were prepared and stained with antibodies against albumin, MFs (F4/80), C5b-9, TNF-α, IL-1β, C3, CD41, Fibrin, P-selectin, STAT3, c-Fos or PDPN. The samples were imaged using a confocal microscope (TCSSP8, Leica). The percentage area of P-selectin and Fibrin expression was measured in mouse liver sections using image J version 1.8.

2.6 | Blood tests

Blood was collected via cardiac puncture without anticoagulant, and serum was separated by centrifugation at 2000 g. Serum AST, bilirubin, ALT, and LDH levels were measured using an automatic chemistry analyzer (Roche Cobas 8000) following standard protocols.

2.7 | Histopathology examination

We fixed, processed, and embedded mouse liver tissue samples in paraffin. After removing the paraffin, we sliced the tissue into sections (5 μm) and stained them with Hematoxylin and eosin (H&E) staining agent (Beyotime product). Next, the sections were labeled with PCNA using immunolabeling. Slice images were captured using a Leica DM2000 microscope. To analyze the liver tissue pathology through optical microscopy, at least two slices were taken from the left lateral lobe of each animal, and the complete slices were qualitatively and quantitatively evaluated to calculate the necrotic area. Quantitative evaluation of the necrotic regions in H&E-stained sections was performed using ImageJ software.

2.8 | Measurement of plasma cytokine levels

Blood was collected from the orbital vein plexus of mice 24 h after APAP administration. The plasma levels of IL-6, TNF-α, and IL-1β were measured using specific ELISA kits according to the manufacturer's instructions.

2.9 | Measurement of thrombin-antithrombin (TAT) complexes in plasma

Peroxidase activity was assessed using the TMB substrate kit (421 101, Biogen) following the manufacturer's instructions. TAT levels in plasma were determined using commercially available enzyme-linked immunosorbent assay (ELISA) kits.

2.10 | Count platelet using flow cytometry

Peripheral blood was collected and treated with PE anti-mouse CD41 antibody. Bead microspheres 3.00 μM (Polysciences) were used as an internal standard for flow cytometry counting.

2.11 | Depletion of platelets

Mice were injected intravenously with a commercially available anti- GPIbα antibody (2 μg/g body weight) for platelet depletion.

2.12 | Polyacrylamide gel electrophoresis (SDS-PAGE) and immunoblotting

Freshly isolated platelets were washed with PBS and re-suspended in a lysis buffer containing protease inhibitors (100 ng/mL, Cell Signaling Technology, Massachusetts, USA). Centrifuge the lysate at 14 000 rpm for 20 min at 4°C and collect the supernatant. After SDS-PAGE, the separated protein was transferred onto a polyvinylidene fluoride (PVDF) membrane and coated with 3% BSA in tris-buffered saline (TBS) at room temperature for 1 h. Incubate the membrane overnight with specific primary antibodies C3 (1:1000), C3aR (1:1000), STAT3 (1:1000), p-STAT3 (Ser232, 1:500), c-Fos (1:1000), and p-c-Fos (Ser 473, 1:500) under 4°C conditions. Incubate the membrane at room temperature in a dark environment for 1 h using goat anti-mouse or goat anti-rabbit antibodies (Licor Odyssey, USA). The membrane was cleaned with TBST (TBS + 0.5% [v/v] Tween-20), and the mixture of an equal volume of solution A with solution B was used to form a chemiluminescent developer, dropped onto the nitrocellulose membrane, and incubated in the dark for 1 min. The photos were developed and obtained using the Tanon 4600SF imaging system. The signal strength was quantified using Image J software.

2.13 | Clearance of macrophage

Following our published methods, mice were intravenously injected with 200 μL of clodronate liposomes

per 20–25 g body weight.[25] Control mice were injected with the liposome control. Depletion efficiency was confirmed by flow cytometry analysis of peripheral monocytes and staining for macrophage using F4/80 antibody and anti-rat Alexa Fluor 488 in liver sections of treated mice.

2.14 | Separation of liver macrophage

The mice were euthanized and perfused through the heart with 10 mL of an infusion solution containing 20 mM Hepes. Immediately afterward, approximately 1.5 g of the mouse liver was finely chopped and incubated in 10 mL of an infusion solution containing 30 mM Hepes, 1 μg/mL Librase TM, and 5 mM $CaCl_2$ in Hank's Balanced Salt Solution (HBSS) solution at 37°C for 30 min. The digestion was stopped by adding 10 mL of HBSS solution containing 2% BSA and 5 mM Ethylenediamine tetraacetic acid (EDTA), and the mixture was passed through a 100 μm mesh filter. Further, isolate nonparenchymal cells by centrifuging at 50 g for 5 min at room temperature. Then, the cells were seeded onto a 0.2% gelatin-coated cover glass in RPMI 1640 in a 24-well plate, supplemented with 10% fetal bovine serum and 100 U/mL penicillin/streptomycin, and incubated for 2 h in a 5% CO_2 atmosphere at 37°C. Non-adherent cells were removed by gently washing them with HBSS, and adherent cells were digested to extract proteins.

2.15 | Luciferase reporter assay

The PDPN gene sequence was cloned into the luciferase reporter vector's Xhol I and Sac I sites (Luc). HEK293T cells were seeded into 24-well dishes and cultured in 10% FBS-supplemented DMEM under 5% CO_2 till 70% confluent. The cells were transiently transfected with 1 mg PDPN pro-Luc or empty-Luc plasmid and 0.4 mg STAT3-pGL4 and c-Fos-pGL4 plasmids using Lipofectamine 3000. The cells were harvested 24 h later, and dual luciferase activity was monitored using a specific kit per the manufacturer's instructions.

2.16 | RNA sequencing

Three male WT mice and three male *C3*$^{-/-}$ mice were injected with APAP. Twenty-four hours later, liver samples were collected, frozen in liquid nitrogen, and stored at −80°C before testing. Total RNA was extracted from tissues using the magnetic bead method, and its quality was analyzed with Agilent 2100 Bioanalyzer electrophoresis. The total RNA was purified using the RNALean assay kit and RNase Free DNase. Next, oligomeric dT beads were used to enrich eukaryotic mRNA, while Ribo ZeroTM magnetic reagent kit was used to remove ribosomal RNA (rRNA) and enrich prokaryotic mRNA. The enriched mRNA was fragmented using fragmented buffer, diluted to a 100 ng/mL concentration, and then reverse transcribed into cDNA using random primers. Double-stranded cDNA was synthesized using dNTP, DNAse I, RNase H, and buffer and then purified using the QiaQuick PCR extraction kit. After the end repair and addition of a poly (A) tail, the fragments were connected to the Illumina sequencing connector and selected by agarose gel electrophoresis. The sequences were amplified by PCR and sequenced by Gene Denovo Biotechnology using the Illumina HiSeq2500 platform. The resulting reads were then cleaned, filtered, and compared against rRNA. Genes/transcripts with FDR parameters below 0.05 and absolute multiple variation R2 were considered differentially expressed genes (DEGs). Primary data analysis included gene annotation, gene expression calibration, and expression correlation analysis. Gene-level differential expression analysis was performed using the Bioconductor R package DESeq2 (v1.22.2), and differential gene heatmaps were generated using the CRAN R package heatmap (v1.0.12). Gene differential expression analysis and Gene Ontology (GO) enrichment analysis were performed on the DEGs. Gene functional enrichment analysis was also conducted using the Gene Set Enrichment Analysis (GSEA) software to generate a GSEA map.

2.17 | Transcript profiling

The RNA-seq data from this study have been deposited in the Genome Sequence Archive in BIG Data Center (https://bigd.big.ac.cn), Beijing Institute of Genomics (BIG), Chinese Academy of Sciences under the accession number: CRA016876 (https://bigd.big.ac.cn/gsa/browse/CRA016876).

2.18 | Statistical analysis

All tests were carried out using GraphPad Prism V8 software. Data were presented as mean ± standard deviation (SD). All data were tested for normality and equal variance. Statistical analyses were conducted using the Mann–Whitney U test for unpaired data or the Wilcoxon

rank test for paired data. Student's t-test or Wilcoxon rank test for paired data, Holm-Šidák test for paired multiple comparison tests, 1-way of variance (ANOVA) for various groups with appropriate post hoc Bonferroni were used. A p value of less than .05 was considered statistically significant.

3 | RESULTS

3.1 | Activation of the C3/C3aR pathway in AILI mice

Complement activation is a biological process involving the complement system that helps enhance the immune system's ability to eliminate pathogens. C3 is the point of convergence of activation pathways, fueling the downstream complement responses.[26] Increased serum complement has been observed among liver diseases, which may be related to inflammation and immune regulatory disorders.[9,11,16] Modulations of the C3/C3 receptor pathway within ALI have not been reported. We first assessed APAP-induced complement activation by measuring the hemolytic activity of serum from APAP-challenged mice. Wild-type (WT) male mice (littermate control mice, 8 weeks old) were intraperitoneally injected with 350 mg/kg of APAP. Twenty-four hours after the injection, serum complement activity increased to 185% (Figure S1A). Since C3aR is one of the activation products of C3 and the primary receptor for C3a, we investigated whether the C3/C3aR pathway participated in liver injury after APAP injection. We observed increased levels of C3 and C3aR mRNA in the livers of these mice compared with those of control mice (Figure S1B,C).

The mRNA levels of the main complement components C1qa, C1qb, and C4b also increased (Figure S1D–F). These observations suggest that the complement system may play an important role in APAP-induced ALI. These results indicated that the C3/C3aR signaling pathway was activated during the AILI.

3.2 | C3 deletion alleviates AILI

To investigate the roles of C3 on ALI, we treated both WT and $C3^{-/-}$ mice with a single dose of APAP at 350 mg/kg and assessed liver damage at various times after the treatment. Further, hepatic GSH levels, which detoxifies NAPQI via conjugation, were similar in the liver sections of both WT and $C3^{-/-}$ mice (Figure 1A), suggesting that there was an equal APAP metabolism in WT and $C3^{-/-}$ mice. At as early as 4 h, serum markers of liver function alanine transferase (ALT) and aspartate aminotransferase (AST) increased in both WT and $C3^{-/-}$ mice. At 12 h, bilirubin also significantly increased, suggesting that both types of mice displayed considerable liver damage shortly after APAP treatment (Figure 1B–D). All markers reached the highest level at 24 h, and their levels in the serum of $C3^{-/-}$ mice were significantly lower than those of WT mice, indicating that C3 deletion alleviated AILI (Figure 1B–D). We further examined the liver histology and found that loss of C3 did not alter the liver histology in healthy mice (Figure 1E–G). Consistent with the serum tests, $C3^{-/-}$ mice showed minimal bleeding or congestion at 24 h when compared with WT mice (Figure 1E–G). Interestingly, introducing recombinant mouse C3 protein (rmC3) into $C3^{-/-}$ mice reversed the protective effects of C3 deletion (Figure 1E–G and Figure S2A,B). We found that the C3 protein did not affect the organs of the mice nor did it cause any inflammatory response (Figure S3). These findings suggest that complement activation is associated with the development of APAP-induced ALI. Hence, inhibiting the activation of the complement system is considered a potential strategy for AILI treatment.

3.3 | C3 functions through its receptor C3aR on the Kupffer cell in AILI

The complement component C3 must be cleaved into two products, C3a and C3b, to exert its biological functions.[27] We hypothesized that the upregulation of C3 would activate liver MFs and their chemotaxis towards liver tissue by binding to C3aR on MFs. Indeed, C3aR expression increased in WT mouse livers upon APAP injection, which was not observed in $C3^{-/-}$ mice nor PBS-treated WT mice (Figure 2A,B). To investigate the properties of MFs expressing C3aR, we conducted phenotype analysis on MFs in the livers of mice with acute injuries.[28] Our research results indicate that most of these MFs comprise Kupffer cells so that future research will focus on liver Kupffer cells (Figure 2C). To explore the effect of C3aR on controlling the function of C3, some $C3aR^{-/-}$ mice were simultaneously treated with rmC3 during the APAP challenge. Further, hepatic GSH levels, which detoxifies NAPQI via conjugation, were similar in the liver sections of both WT and $C3aR^{-/-}$ mice (Figure 2D). In contrast to WT mice, $C3aR^{-/-}$ mice exhibited lower serum ALT levels and reduced liver injury at 24 h following APAP injection, and rmC3 did not show any effect on AILI among $C3aR^{-/-}$ mice

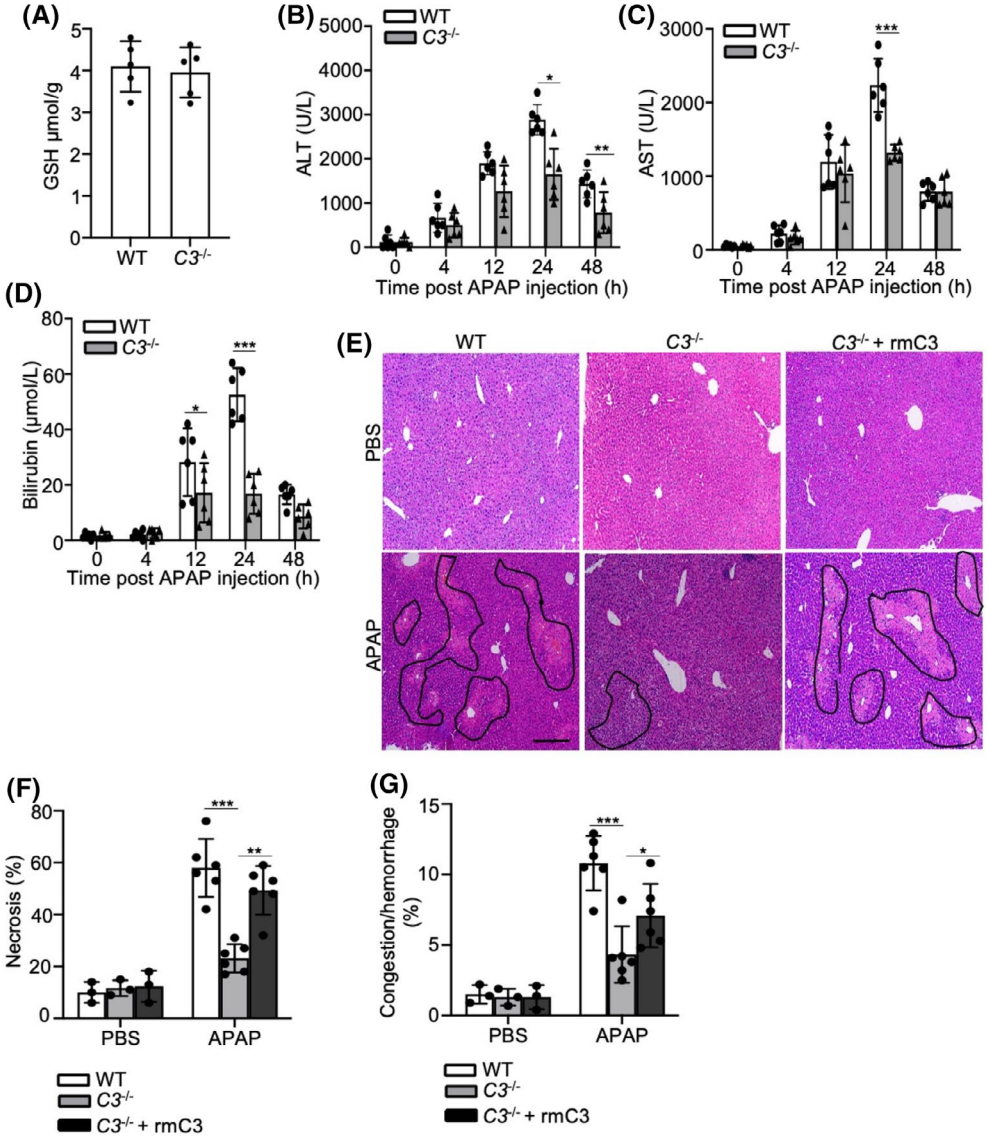

FIGURE 1 C3 deficiency alleviates AILI. (A) Hepatic GSH levels in WT and $C3^{-/-}$ mice at 0 h time point. (B–D) Wild-type (WT) and $C3^{-/-}$ mice (male, eight weeks old, $n = 4$–8/group) received a single dose of APAP at 350 mg/kg. Mouse serum was collected at various times after APAP injection and tested for four markers: Alanine transferase (ALT), aspartate aminotransferase (AST), and bilirubin. (E–H) Male WT and $C3^{-/-}$ mice were subjected to APAP treatment as described above. Additionally, $C3^{-/-}$ mice were separated into two groups ($n = 5$–6/group) and treated with either PBS or recombinant mouse C3 (i.p., 500 ng/ mouse) immediately after APAP injection. Twenty-four hours after the injection, mouse livers were harvested and subjected to examinations. (E) Representative illustrative images of H&E-stained liver sections. The outlined are necrotic areas. Scale bar, 20 μm. (F) Quantification of areas of hepatocellular necrosis. (G) Quantification of hepatic congestion and hemorrhage areas were determined 24 h after the APAP challenge. Data were mean ± SD of at least 3 independent experiments and were analyzed using 1-way ANOVA followed by Tukey's test for multiple groups and were representative of 3 independent experiments. Statistical significance was represented by asterisks, *$p < .05$. **$p < .01$. ***$p < .001$.

(Figure 2E). $C3aR^{-/-}$ mice showed minimal bleeding or congestion at 24 h compared to WT mice (Figure 2F–H). As expected, C3aR deficiency also notably inhibited C3 activation and the deposition of MAC in the liver, and rmC3 similarly did not affect MAC deposition in the liver (Figure 2I). These results demonstrated the critical role of C3aR in mediating C3-induced liver injury in the context of APAP-induced hepatotoxicity.

3.4 | The C3/C3aR pathway contributes to AILI by promoting Kupffer cell-dependent platelet recruitment to the liver

Thrombocytopenia often occurs in patients with excessive APAP.[1,29] It may be related to platelets recruitment into the liver. Compared with $C3^{-/-}$ mice, APAP

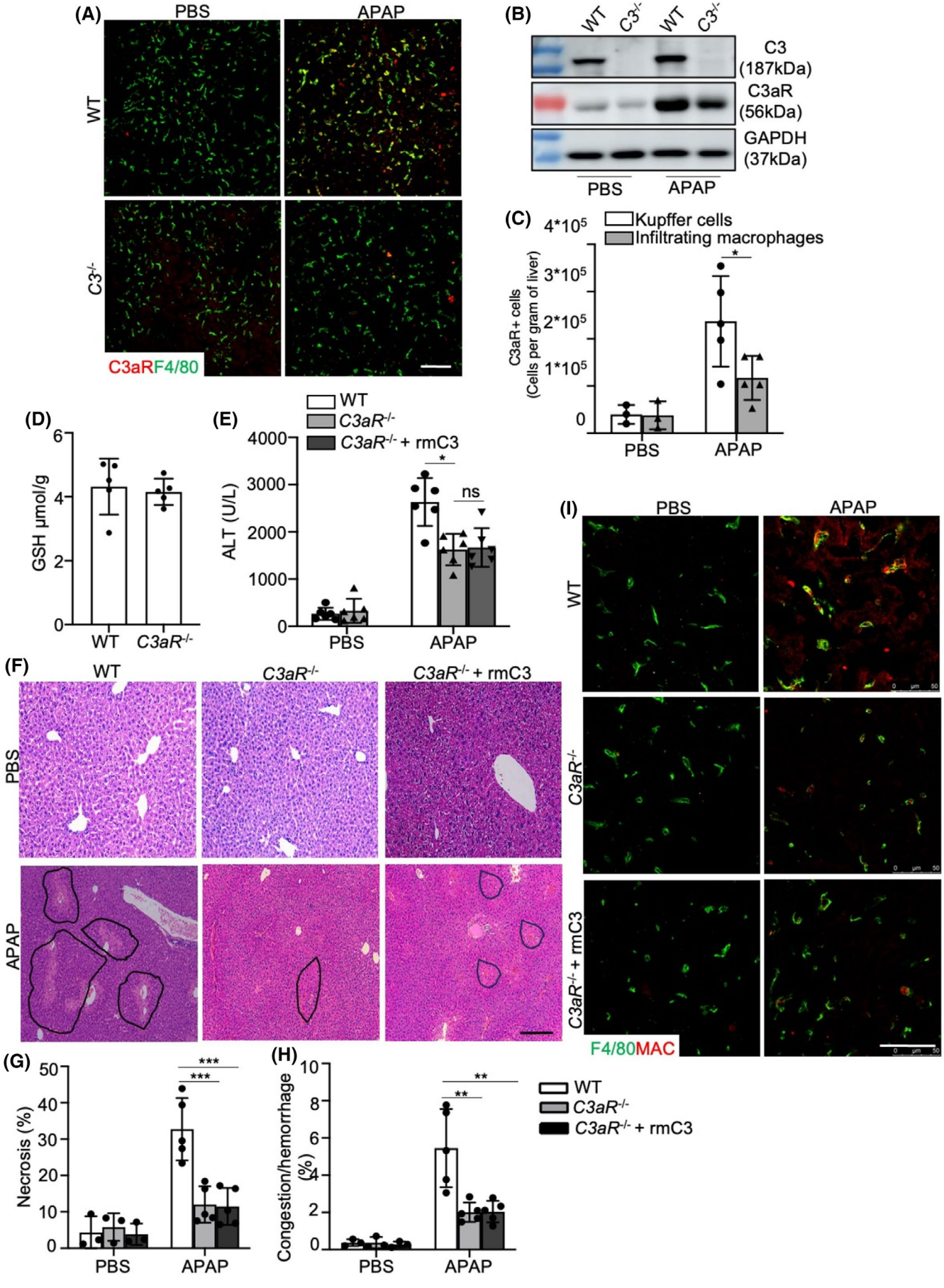
(A)
PBS
APAP
WT
C3-/-
C3aRF4/80
(B)
WT
C3-/-
WT
C3-/-
C3 (187kDa)
C3aR (56kDa)
GAPDH (37kDa)
PBS
APAP
(C)
Kupffer cells
Infiltrating macrophages
C3aR+ cells (Cells per gram of liver)
4*10^5
3*10^5
2*10^5
1*10^5
0
*
PBS
APAP
(D)
GSH μmol/g
6
4
2
0
WT
C3aR-/-
(E)
WT
C3aR-/-
C3aR-/- + rmC3
ALT (U/L)
4000
3000
2000
1000
0
*
ns
PBS
APAP
(F)
WT
C3aR-/-
C3aR-/- + rmC3
PBS
APAP
(I)
PBS
APAP
WT
C3aR-/-
C3aR-/- + rmC3
F4/80MAC
(G)
Necrosis (%)
50
40
30
20
10
0
***
***
PBS
APAP
(H)
Congestion/hemorrhage (%)
10
8
6
4
2
0
**
**
PBS
APAP
WT
C3aR-/-
C3aR-/- + rmC3

FIGURE 2 C3 contributes to AILI through its receptor C3aR on Kupffer cells. (A and B) WT and $C3^{-/-}$ mice ($n = 6$/group) received either PBS or 350 mg/kg of APAP, and their livers were collected for immunofluorescence analysis (A) and western blotting (B) at 24 h after the injection. The images showed C3aR (red) and F4/80 (green) double-positive cells in the livers and C3 and C3aR protein levels in the liver lysates. Scale bars = 10 μm. (C) In another group, livers were extracted, digested, and C3aR-expressing infiltrating macrophages (defined by the gating strategy CLEC4F$^-$F4/80$^+$) and resident Kupffer cells (defined by the gating strategy CLEC4F$^+$F4/80$^+$) were isolated, quantified by flow cytometry and expressed as the number of cells per gram of liver tissue. $n = 6$. (D) Hepatic GSH levels in WT and $C3aR^{-/-}$ mice at 0 h time point. (E–H) Male WT and $C3aR^{-/-}$ mice ($n = 5$/group) were treated with either APAP or PBS. A group of $C3aR^{-/-}$ mice were treated with both APAP and recombinant mouse C3 (rmC3). Twenty-four hours after the treatment, blood and livers were collected for analysis. (E) Serum levels of ALT. (F) Representative images of H&E-stained livers demonstrating the necrotic areas (outlined). Scale bar, 20 μm. (G) Quantification of areas of hepatocellular necrosis. (H) Quantification of hepatic congestion and hemorrhage areas were determined 24 h after APAP challenge. (I) Representative immunofluorescent images showing MAC complex in the livers. Scale bars = 50 μm. Data represents mean ± SD from at least 3 independent experiments and were analyzed using one-way ANOVA followed by Tukey's test for multiple groups and is representative of 3 independent experiments. Statistical significance is denoted by asterisks as follows: *$p < .05$.

stimulation induces more severe thrombocytopenia in WT mice (Figure 3A). At 24 h after APAP treatment, compared with $C3^{-/-}$ mice, there was apparent platelet aggregation in the WT liver, and approximately 90% of these platelet aggregates were found on the surface of Kupffer cells (Figure 3B). According to the reports, depleting platelets before APAP injection can prevent liver damage in mice. Therefore, we treated WT mice with anti-CD41 antibody before APAP injection and confirmed that the pretreatment reduced platelet concentration in circulation by over 75% compared to control IgG-pretreated mice (Figure 3C). Our results suggest that platelet depletion could mitigate AILI (Figure 3D) without affecting the expression of liver C3 (Figure 3E), implying that C3/C3aR regulates platelet-mediated AILI. To investigate the role of C3aR in mediating C3 function, $C3aR^{-/-}$ mice were treated with rmC3 simultaneously with APAP. Results showed that rmC3 caused no difference in platelet recruitment in $C3aR^{-/-}$ mice (Figure 3F). This contrasts the results showing restored platelet accumulation and increased AILI in $C3^{-/-}$ mice treated with rmC3. These results indicated that C3aR played a critical role in C3-mediated liver platelet accumulation and AILI.

To further understand the role of Kupffer cells in APAP-induced complement-regulated platelet recruitment to the liver and the effects on AILI, we depleted Kupffer cells before APAP injection and then accessed liver injury. We improved a reported clodronate (CLDN) treatment-based method[1] for MF removal, and Figure 4A confirmed that at 20 h after CLDN treatment, MFs (both resident Kupffer cells and infiltrating MFs) in mouse livers were completely depleted. Consistent with the reports in the literature, after treatment with CLDN, the expression of C3aR is significantly reduced in liver (Figure S4).[30] C3aR mRNA is very highly expressed in Kupffer cells while present in low levels in hepatocytes and total liver. This lack of MFs significantly reduced C3-mediated AILI (Figure 4B,C) and platelet accumulation in the livers (Figure 4D). Consistent with this, platelet P-selectin staining was reduced in C3-deficient mice (Figure S5A,B). These results indicate that hepatic Kupffer cells played a pivotal role in recruiting platelets into the liver through C3, thus promoting AILI.

3.5 | Kupffer cells promote platelet recruitment through CLEC-2/PDPN interaction

Monocyte PDPN plays an important role in complement activation, which is triggered by liver dysfunction during inflammation.[20] To further investigate the role of the C3/C3aR signaling pathway in Kupffer cell-mediated platelet recruitment to the liver, we measured the expression of PDPN in Kupffer cells, which is crucial for platelet recruitment. In uninjured mice, PDPN was expressed in the liver at a minimal level.[31] However, APAP increased hepatic PDPN expression in mice, and the increase was C3 and C3aR dependent (Figure 5A,B). We found that the C3 protein alone did not affect the expression of PNPN in $C3^{-/-}$ mice or $C3aR^{-/-}$ mice, but after injection APAP, C3 protein induced the expression of PDPN in liver (Figure S6A,B). To study the role of PDPN in AILI, we generated myeloid cell PDPN-deficient mice (LysM $Pdpn^{-/-}$). Deletion of PDPN in Kupffer cells significantly reduced serum ALT activity and liver damage compared to WT control mice 24 h after APAP treatment (Figure 5C,D), when APAP-induced liver damage was at the peak. Additionally, compared with WT mice, fewer platelets were sequestered to Kupffer cells in the hepatic tissues of LysM $Pdpn^{-/-}$ mice (Figure 5E).

PDPN is exclusively recognized by CLEC-2, the sole identified platelet receptor with binding capabilities to PDPN.[32] To investigate the effect of PDPN on platelet adhesion to liver Kupffer cells, we generated mice with specific deletion of platelet CLEC-2, Plt $Clec\text{-}2^{-/-}$.

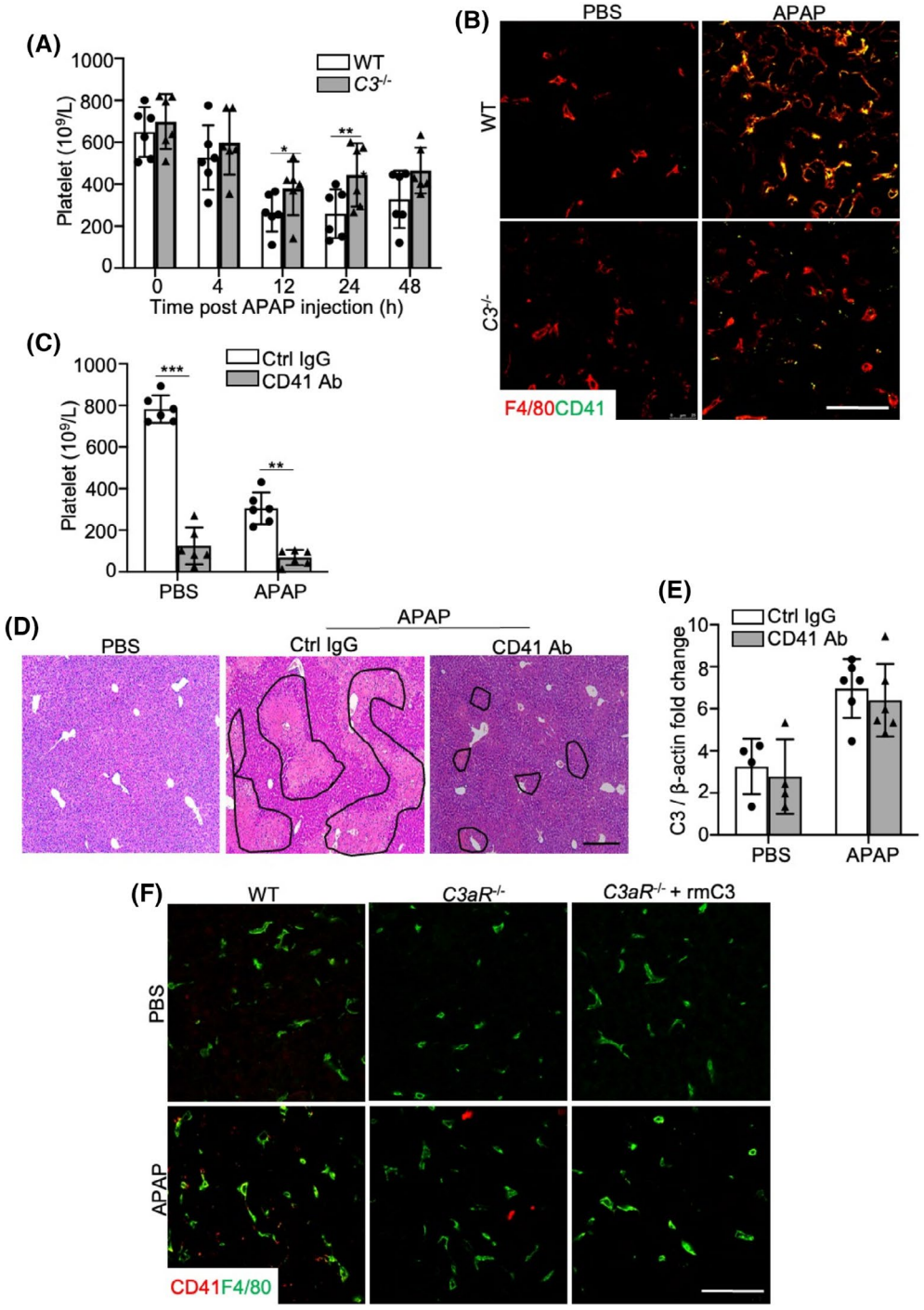

FIGURE 3 C3/C3aR Regulates AILI by promoting platelet recruitment to the liver. (A) Male WT and $C3^{-/-}$ mice were injected intraperitoneally with 350 mg/kg APAP. Peripheral blood was collected before and at various time points after infection, treated with PE anti-mouse CD41 antibody, and platelet count was measured with Hemavet®. (B) Representative confocal images of frozen liver sections of liver from WT and $C3^{-/-}$ mice. The livers were collected 24 h post-APAP injection, and the sections were labeled with anti-CD41 (green) and anti-F4/80 (red) antibodies. Scale bar, 50 μm. (C–E) Male WT mice were administered with control IgG (Ctrl IgG) or an anti-CD41 antibody (CD41 Ab) 4 h before APAP or PBS administration for platelet depletion. (C) Peripheral blood was collected 8 h after APAP infection, and platelet count was measured with Hemavet®. (D) Livers were collected for histology examination 24 h after APAP treatment. Necrotic areas were outlined in the representative images of H&E-stained liver sections. $n = 5$ mice/group. Scale bar, 20 μm. (E) Level of C3 transcripts in the livers were accessed with RT-qPCR. The measurements were normalized with β-Actin expression. (F) WT and $C3aR^{-/-}$ mice were treated with rmC3 simultaneously with APAP. The livers were collected 24 h after the injections, and the liver sections were labeled with anti-CD41 (red) and anti-F4/80 (green) antibodies. Representative confocal images are shown here. Scale bar, 50 μm. $n = 5$ mice/group. Data represents mean ± SD from at least 3 independent experiments and were analyzed using one-way ANOVA followed by Tukey's test for multiple groups and were representative of 3 independent experiments. Statistical significance is denoted by asterisks: $^*p < .05$, $^{**}p < .01$, $^{***}p < .001$.

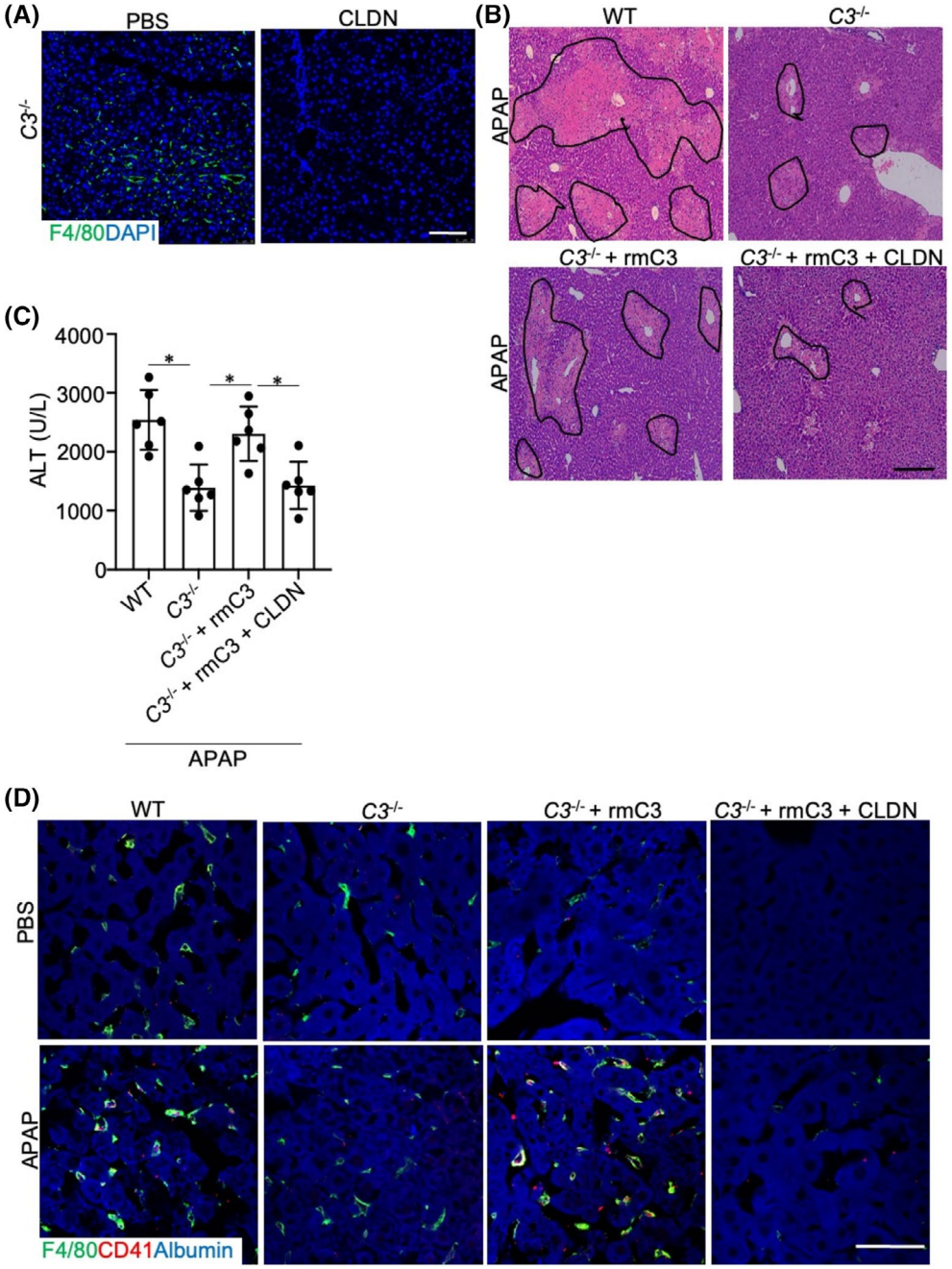

FIGURE 4 C3 deficiency in ameliorating hepatic injury is hepatic macrophage dependent. (A) $C3^{-/-}$ mice were injected with either empty liposomes containing either PBS or clodronate (CLDN) 10 h before APAP treatment. Livers were collected at 24 h after APAP injection, and liver sections were labeled with anti-F4/80 (green) and DAPI (blue). Representative confocal images were shown. Scale bar, 10 μm. $n = 6$ mice/group. (B–D) After injection with PBS or CLDN, WT and $C3^{-/-}$ mice were treated with APAP. Additionally, $C3^{-/-}$ mice were divided into two groups treated with either PBS or rmC3 simultaneously with APAP. At 24 h after APAP treatment, blood and livers were collected for analyses. (B) Representative images of H&E-stained liver sections with necrotic areas outlined. $n = 6$ mice/group. Scale bar, 20 μm. (C) Serum levels of ALT. (D) Representative confocal images of liver sections stained with anti-CD41 (green) and anti-F4/80 (red) antibodies. Scale bar, 50 μm. $n = 6$ mice/group. Data represents mean ± SD from at least 3 independent experiments and were analyzed using 1-way ANOVA followed by Tukey's test for multiple groups and were representative of 3 independent experiments. Statistical significance is denoted by asterisks as follows: $^*p < .05$.

Compared with WT mice, Plt *Clec-2*$^{-/-}$ mice we had significantly less liver damage 24 h after APAP injection, reflected by lower serum ALT levels (Figure 6A) and smaller necrotic areas (Figure 6B). Deletion of platelet CLEC-2 abolished platelet recruitment into the liver (Figure 6C), indicating that CLEC-2 contributes to AILI by mediating platelet recruitment to the liver. However, deficiency of neither platelet CLEC-2 nor myeloid

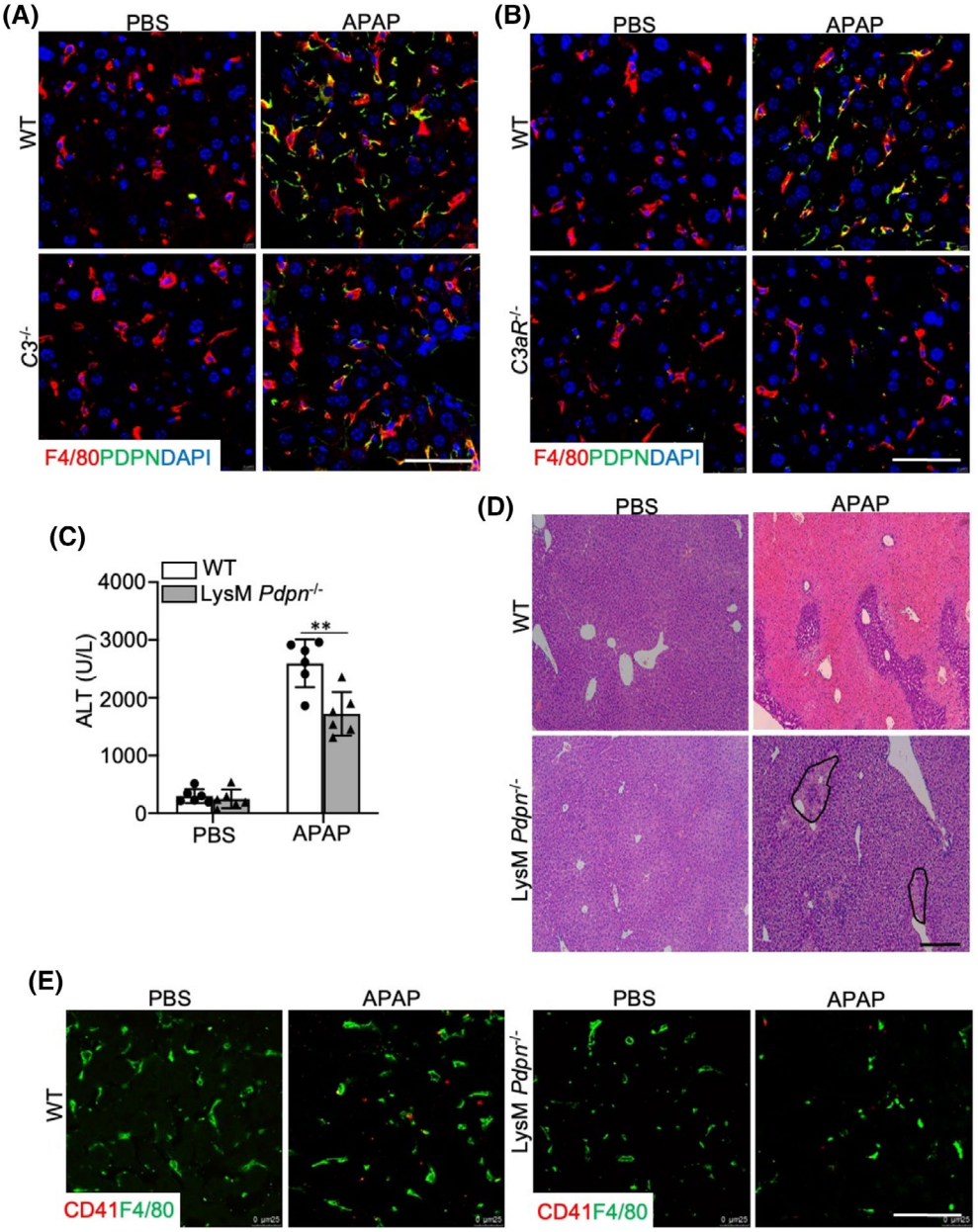

FIGURE 5 Contribution of C3/C3aR signaling to the upregulation of podoplanin expression in macrophage and to platelet adhesion. (A and B) Representative confocal images of frozen liver sections stained with anti-PDPN (green) and anti-F4/80 (red) antibodies. Livers were collected from WT, $C3^{-/-}$, and $C3aR^{-/-}$ mice at 24 h after they were treated with APAP. Scale bar, 50 μm. $n = 5$ mice/group. (C and D) WT and LysM $Pdpn^{-/-}$ mice were treated with APAP. At 24 h after the treatment, blood and livers were collected for serum ALT measurement and liver histology study, respectively. In the representative images of H&E-stained liver sections, the necrotic areas were outlined. $n = 6$ mice/group. Scale bar, 20 μm. (E) Representative confocal images of frozen liver sections from WT and LysM $Pdpn^{-/-}$ mice stained with anti-CD41 (red) and anti-F4/80 (green) antibodies. The livers were collected at 24 h post-APAP or saline injection. $n = 6$ mice/group. Scale bar, 50 μm. Data represents mean ± SD from at least 3 independent experiments and were analyzed using 1-way ANOVA followed by Tukey's test for multiple groups and were representative of 3 independent experiments. Statistical significance is denoted represented by asterisks as follows: $^{**}p < .01$.

cell PDPN affected the level of C3 in the mouse livers (Figure 6D,E), suggesting that the C3/C3aR pathway influences the liver PDPN/CLEC-2 interaction, rather than the reverse. In summary, our data elucidated that liver Kupffer cells recruit platelets via PDPN-CLEC-2 interaction, and PDPN expression on Kupffer cells was modulated by C3/C3aR signaling.

3.6 | C3 upregulates PDPN expression in hepatic Kupffer cells by activating the STAT3/c-Fos pathway in AILI

Abnormal activation of inflammation signaling pathways contributes to the progression of AILI.[33] We conducted RNA sequencing to profile the transcriptomes

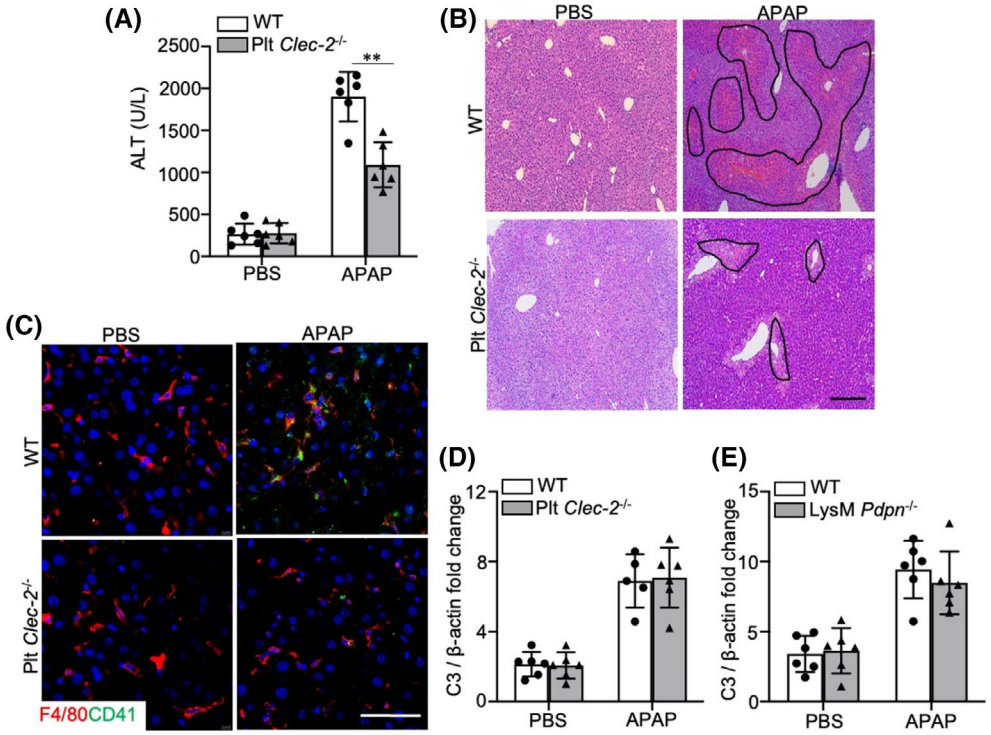

FIGURE 6 Hepatic macrophages recruit platelets through CLEC-2/PDPN interaction. (A and B) Serum levels of ALT and liver histology were assessed 24 h after APAP treatment. In the microscopic images of H&E-stained liver sections, necrotic areas were outlined. $n = 6$ mice/group. Scale bar, 20 μm. (C) Representative confocal images of frozen sections of liver from WT and Plt *Clec-2*$^{-/-}$ mice stained with anti-CD41 (red) and anti-F4/80 (green) antibodies at 24 h after injection of APAP or saline. Scale bar, 50 μm. (D and E) Levels of C3 transcripts in the livers of Plt *Clec-2*$^{-/-}$, LysM *Pdpn*$^{-/-}$ and WT mice after 24 h of APAP administration. The measurements were normalized with GAPDH expression. $n = 6$ mice/group. Data represents mean ± SD from at least 3 independent experiments and was analyzed using one-way ANOVA followed by Tukey's test for multiple groups and were representative of 3 independent experiments. Statistical significance is denoted by asterisks as follows: $^{**}p < .01$.

of the livers from *C3*$^{-/-}$ and WT littermates collected 24 h after APAP injection and compared their gene expression patterns using principal components analysis. To further investigate the mechanisms underlying C3 regulation of PDPN expression in hepatic Kupffer cells, we screened for downregulated transcription factors in *C3*$^{-/-}$ livers that could potentially regulate PDPN (Figure 7A). We identified E2f3, Arntl, Ahr, Runx1, c-Fos, STAT3, and HNF1 as the potential regulators (Figure 7B). Intercellular contact enhances the activation of the epidermal growth factor receptor (EGFR) and the signaling activator STAT3, leading to increased PDPN expression and the promotion of squamous cell carcinoma motility.[34] Therefore, we focused on the STAT3/c-Fos pathway. We found over 400 significantly enriched proteins, including components of multiple transcriptional complexes such as STAT3 and c-Fos (Figure 7C). Motif analysis was performed on all common PDPN-binding loci and the high-confidence STAT3 and c-Fos-regulated enhancers. The study confirmed the presence of PDPN-binding sites upstream of the STAT3- and the c-Fos-expressing cassettes, respectively (Figure 7D), suggesting that STAT3 and c-Fos are also targets TF of PDPN. PDPN should be the target of these two transcription factors. To determine whether PDPN is a target gene of STAT3 and c-Fos, we conducted luciferase reporter gene assays, which confirmed the interaction between STAT3 and the PDPN promoter and the interaction between c-Fos and the promotor. When the reporter gene was placed under the control of the PDPN promoter, luciferase activity increased upon co-transfection with either STAT3- or c-Fos-expressing vectors (Figure 7E,F).

Although we found that the formation of transcription complexes of c-Fos and STAT3 plays a crucial role in the induction of PDPN gene expression after APAP stimulation, it's still uncertain how the expression levels of c-Fos/STAT3 are involved in inflammation-driven PDPN gene expression. To determine whether phosphorylation of c-Fos/STAT3 is crucial for APAP-induced PDPN expression, we examined the phosphorylation of c-Fos/STAT3 in liver MFs of WT and *C3*$^{-/-}$ mice. The results indicate that APAP leads to enhanced phosphorylation of c-Fos/STAT3 in liver Kupffer cells of WT mice. However, APAP

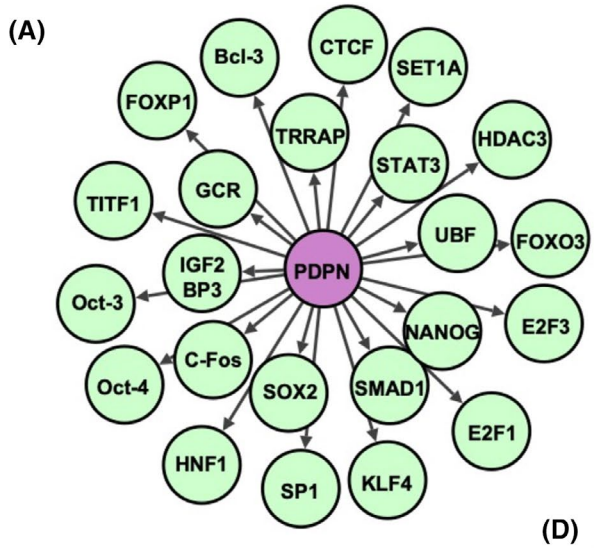

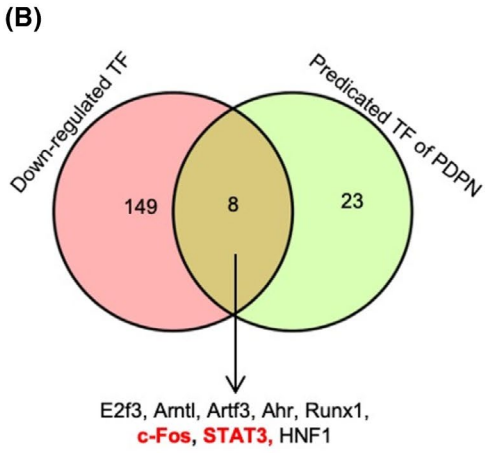

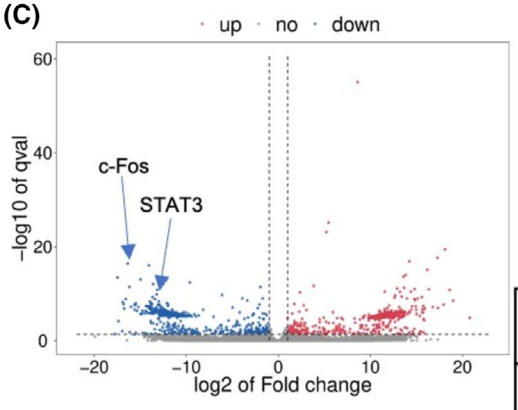

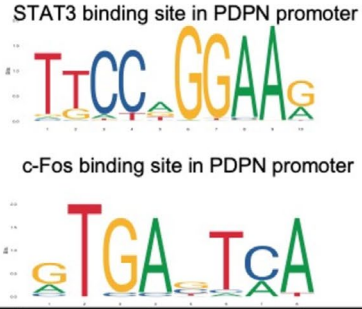

Name	Score	Relative score	Start	End	Predicted sequence
STAT3	12.671319	0.92	967	976	TTCCAGGAAT
c-Fos	14.470551	0.92	325	332	GTGATTAA

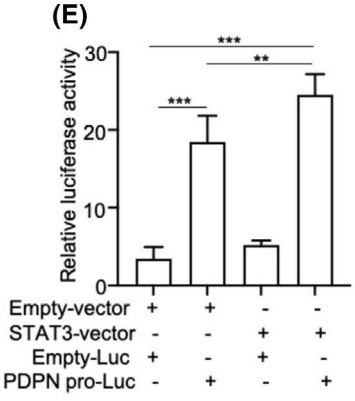

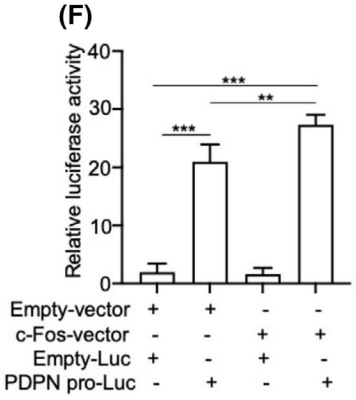

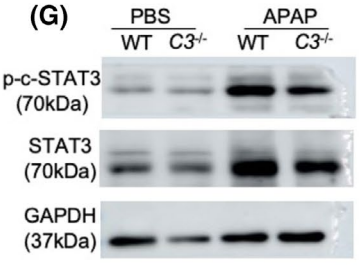

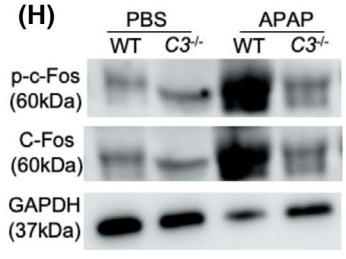

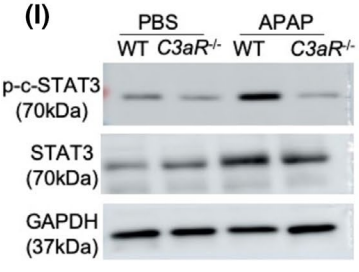

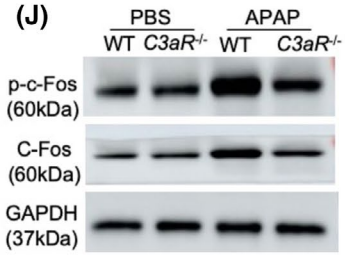

FIGURE 7 C3 upregulates PDPN expression in hepatic MFs via activating STAT3/c-Fos in AILI. (A–D) WT and $C3^{-/-}$ mice (male, $n = 3$/group) were injected with APAP. Twenty-four hours later, mouse livers were collected and the extracted total RNAs were used for sequencing and data analysis. (A) Transcription factors (TFs) targeting PDPN were predicted using the PROMO ALGGEN database within a dissimilarity margin less than or equal to 5%. (B) Venn diagram depicting downregulated TFs in $C3^{-/-}$ livers (in comparison with WT livers) and predicted TFs of PDPN in the livers. The number of congruently downregulated genes is indicated in the middle, and their gene symbols are listed at the bottom. (C) Volcano plot of illustrating differentially expressed genes between APAP-treated WT and $C3^{-/-}$ mice. Red, significantly upregulated genes (log2 fold-change >1.5); blue, significantly downregulated genes (log2 fold-change <1.5). c-Fos and STAT3 are highlighted. (D) Prediction of STAT3 and c-Fos-binding elements on the promoters of PDPN through JASPAR. (E and F) HEK293T cells were transfected with either control vector (control), STAT3-, or c-Fos-expressing vectors. The cells were also co-transfected with luciferase-expressing vectors with or without PDPN promoter (PDPN-Luc or Luc). Luciferase activity levels were then measured. $n = 9$. (G–J) Immunoblots depicting levels of phosphorylated STAT3 (p-STAT3), STAT3, phosphorylated c-Fos (p-c-Fos), and c-Fos in liver macrophages from mice 24 h after PBS or APAP injection. Data represents mean ± SD from at least 3 independent experiments and were analyzed using one-way ANOVA followed by Tukey's test for multiple groups and were representative of 3 independent experiments. Statistical significance is denoted by asterisks as follows: $^{**}p < .01$, $^{***}p < .001$.

upregulated the STAT3/c-Fos pathway in the liver Kupffer cells, which was reversed in $C3^{-/-}$ mice (Figure 7G,H). Next, we examined the phosphorylation of c-Fos/STAT3 in liver MFs of WT and $C3aR^{-/-}$ mice. The results indicate that APAP leads to enhanced phosphorylation of c-Fos/STAT3 in liver Kupffer cells of WT mice. However, APAP upregulated the STAT3/c-Fos pathway in the liver Kupffer cells, which was reversed in $C3aR^{-/-}$ mice (Figure 7I,J). We used siRNA to knock down C3aR in the RAW264.7 cell line, and treated the cells with LPS while adding C3 protein. We then assessed the phosphorylation levels of STAT3 and c-FOS. The results showed that the lack of C3/C3aR interaction inhibited the phosphorylation of STAT3 and c-FOS (Figure S7A–C).

Overall, our results indicated that the C3/C3aR signaling pathway upregulated PDPN expression in liver Kupffer cells through c-Fos and STAT3, which directly bound to the promoter region of PDPN.

3.7 | C3 deletion reduces the release of inflammatory factors by Kupffer cells, thereby alleviating liver injury and coagulation

Pro-inflammatory cytokines play a crucial role in the pathogenesis of AILI. Among cytokine derived from macrophages, TNF-α and IL-1β play important roles in the occurrence and aggravation of liver injury.[35,36] To investigate the role of C3 in inflammation, we examined the levels of cytokines in both plasma and livers of APAP-treated mice. Plasma levels of TNF-α, IL-6, and IL-1β were significantly lower in $C3^{-/-}$ mice compared with those of WT mice 24 h after APAP injection (Figure 8A–C), suggesting that C3 exerts an enhancing effect on the systemic proinflammatory response induced by APAP. In the livers of both APAP-treated WT and $C3^{-/-}$ mice, levels of TNF-α as well as IL-1β transcripts were increased at 4 h after APAP treatment (Figure 8D,E). However, at 24 h, the levels in $C3^{-/-}$ mice were significantly lower than in WT mice (Figure 8D,E). Expression of TNF-α and IL-1β proteins in the livers at 24 h post-injection exhibited a similar pattern, where they partially co-localized with Kupffer cells (Figure 8F,G). Hence, C3 deficiency attenuated inflammation in the liver during AILI. Plasma TAT levels were affected only at 6 h post-APAP in $C3^{-/-}$ mice, suggesting an early and transient contribution of complement to the generation of thrombin after APAP overdose (Figure 8H). These results showed that C3 deletion can reduce the inflammation in APAP-induced liver injury.

4 | DISCUSSION

This study demonstrated the critical roles of C3/C3aR in developing AILI. In APAP-treated mice, C3/C3aR signaling upregulated the expression and phosphorylation of transcription factors STATs and c-Fos in hepatic Kupffer cells, which in turn increased PDPN expression, promoting platelet recruitment to the Kupffer cells via the interaction of PDPN and the CLEC-2 on platelets.

It was reported that drug-metabolizing enzymes are different in female mice. Female mice are more sensitive to the toxicological effects of APAP than male mice, which may be due to the higher production rate of reactive metabolites and their direct interaction with glutathione, thereby reducing the liver content of this tripeptide.[37]

Excessive APAP metabolism in the liver can lead to spontaneous damage to liver cells, releasing danger signals and activating innate immune responses. This triggers aseptic inflammation, further worsening liver damage.[38,39] The present study investigated the involvement of the complement system in AILI and explored the therapeutic potential of targeting the C3/C3aR pathway. Coagulation, inflammation, and complement activation

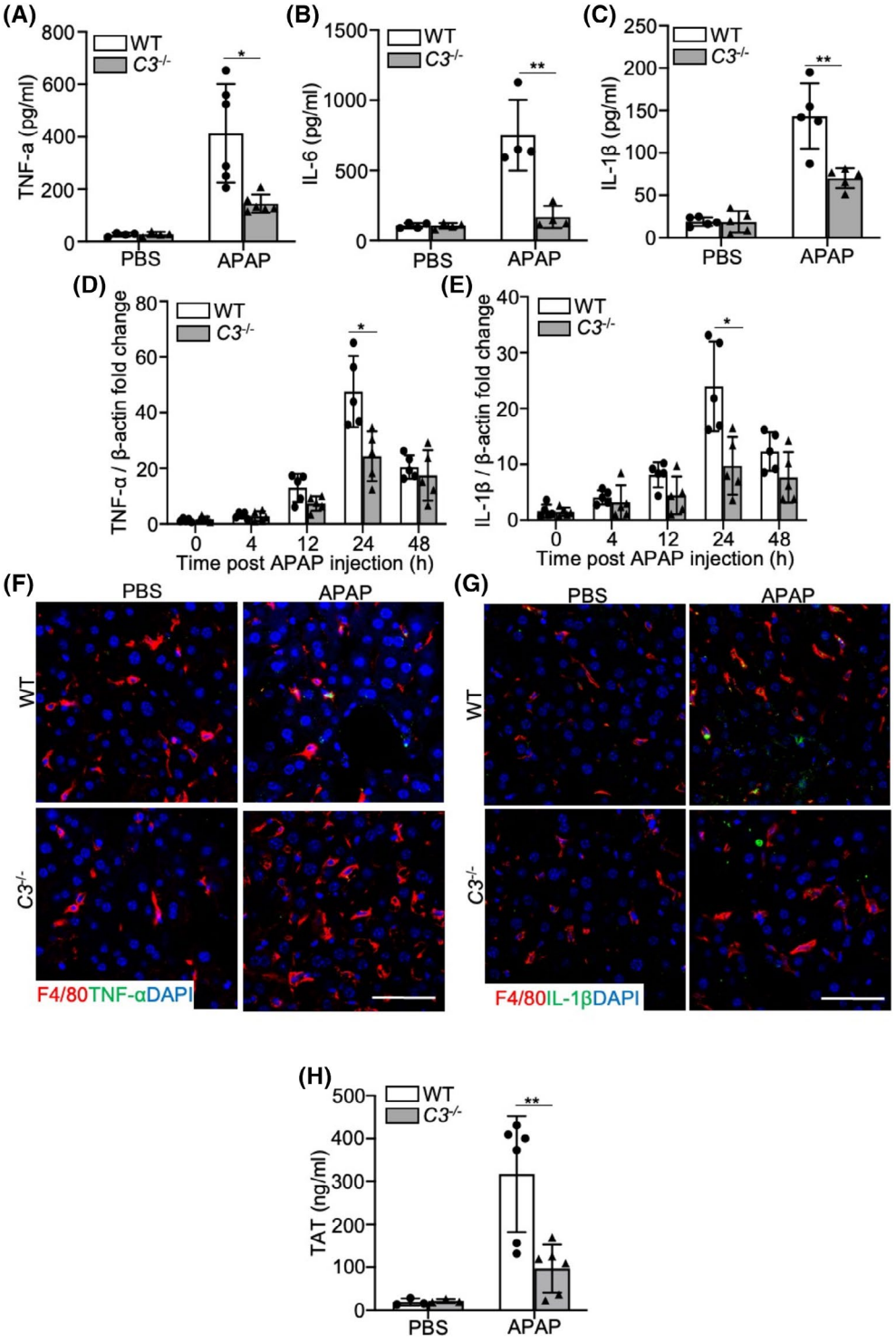

FIGURE 8 C3 deficiency reduces APAP-induced liver inflammation. $C3^{-/-}$ and their littermate control mice were treated with a single dose of either PBS (control) or APAP, and mouse plasma and livers were collected for analysis. (A–C) Plasma levels of TNF-α, IL-1β, and IL-6 at 8 h after the treatment. (D and E) Levels of TNF-α and IL-1β transcripts in the livers measured using RT-qPCR. The measurements were normalized with GAPDH expression. $n = 9$ mice/group. (F and G) Illustrative immunofluorescent images of liver cryosections at 24 h after injection. $n = 6$ mice/group. Scale bar: 50 μm. (H) Determination of Thrombin-antithrombin complex (TAT) plasma levels in wild-type and $C3^{-/-}$ mice by ELISA. $n = 6$ mice/group. Data represents mean ± SD from at least 3 independent experiments, analyzed using one-way ANOVA followed by Tukey's test for multiple groups, and is representative of 3 independent experiments. Statistical significance is denoted by asterisks as follows: $^{*}p < .05$, $^{**}p < .01$.

collectively contribute to liver injury.[40] Inhibiting complement activation can reduce coagulation activation and ameliorate systemic inflammatory responses within 24 h, thus protecting liver function from inflammation-induced liver injury.[41] Uncontrolled complement activation can lead to cell death and organ damage during inflammation.[19] While excessive complement activation has been shown to worsen AILI,[26] it is currently unclear whether activated complement products mediate platelet activation and exacerbate liver injury. One significant finding of this study is that in AILI, the activation of the C3/C3aR signaling pathway aggravates liver injury through Kupffer cell activation and its interaction with platelets. Our research presents convincing evidence indicating that C3 interacts with its receptor C3aR on Kupffer cells, promoting platelets recruitment to Kupffer cells, thereby leading to AILI. C3 can interact with multiple receptors, which aligns with its diverse functions in various disease contexts. One study showed that the abnormally activated microglia exacerbated white matter injury during chronic hypoperfusion via the C3/C3aR pathway.[42] Our study elucidates the pivotal role of the C3/C3aR pathway in liver platelet recruitment and its impact on AILI. By using $C3^{-/-}$ and $C3aR^{-/-}$ mice in our experiments, we demonstrated that C3aR is the mediator of C3 action in AILI. We observed that C3 primarily binds to C3aR on Kupffer cells rather than other C3aR-expressing liver cells, which warrants further investigation.

Kupffer cells are involved in the occurrence and development of various liver diseases, including ALI.[43] Recent reports have also shown that dysfunction of Kupffer cells can lead to fibrosis and cell death, and apoptosis is a common response of liver Kupffer cells to toxic damage.[44] C3aR mRNA is very highly expressed in Kupffer cells while present in low levels in hepatocytes and total liver.[30] C3 primarily binds to C3aR on hepatic Kupffer cells, rather than other cells expressing C3aR in the liver, suggesting two possibilities that warrant further investigation. Firstly, C3 may bind to a specific subtype of C3aR uniquely expressed on Kupffer cells. Secondly, the interaction between C3 and C3aR may require a co-receptor that is expressed on Kupffer cells but not on other C3aR-expressing cells in the liver. After CLDN treatment, hepatic macrophages are depleted, and although APAP upregulates the expression of C3aR on other liver cells, the interaction between C3 and macrophage C3aR is inhibited. This indicates that hepatic macrophages, including Kupffer cells and infiltrating monocytes, play a crucial role in promoting hepatic platelet accumulation, thereby contributing to APAP-induced liver injury. Earlier research employing CLDN to deplete Kupffer cells has suggested that Kupffer cell depletion exerts a protective effect against AILI,[45] which is consistent with our results. According to reports, injecting CLDN about 40 h before APAP treatment resulted in an increase in the number of MFs in the liver during APAP treatment, leading to the conclusion in published reports that KCs have a protective effect on AILI.[46] However, another scenario is that the worsening of damage may be due to increased infiltrating macrophages and platelet accumulation. To better investigate the role of liver MFs in platelet recruitment, we established a time period after CLDN treatment in which both KCs and infiltrating macrophages were absent, based on an improved method in recent research.[1] Our data indicates that when the Kupffer cell and infiltrating macrophages population are absent in the liver, there is no apparent APAP-induced platelet recruitment to the liver, and the mice exhibit less severe liver injury than those without Kupffer cell depletion. In summary, these results indicate that liver Kupffer cells exert an important effect on the promotion of hepatic platelet accumulation, thereby contributing to AILI.

Our study focused on the interaction between platelet CLEC-2 and PDPN on Kupffer cells and its impact on C3 signaling pathways during liver injury caused by APAP. C5b9 is known for its ability to disrupt cell membranes, leading to cell lysis and death, which can exacerbate liver injury. We found that C3aR deficiency notably inhibited C3 activation and the deposition of C5b9 in the liver, and rmC3 similarly did not affect C5b9 deposition in the liver. Complement activation ultimately functions through the formation of the C5b9 complex, with C3 as an intermediate step. All three pathways of complement activation ultimately activate C3, which then transmits signals downstream, making C3 upstream of C5b9. This study involves blocking the C5b9 signal upstream in the signaling pathway. Additionally, the C3/C3aR signaling pathway also regulates the interaction between liver macrophage PDPN and platelet CLEC-2. Inflammation, coagulation, and complement cross-interact with each other and contribute to liver injury differentially at the different stages of ALI. Inhibition of complement activation reduces coagulation activation and ameliorates systemic inflammatory responses within 24 h in a primate model of ALI, which protects liver function as a consequence.[41] Uncontrolled complement activation causes cell death and organ damage in ALI.[19] Our results not only are consistent with a primate study that shows inhibition of complement C3 and C5 protects liver function[14] but also provide mechanistic insights into the pathological consequences of the activated complement in ALI. Our research has revealed a new role of the C3/C3aR axis in AILI and extensively investigated the mechanism through which C3/C3aR signaling facilitates platelet accumulation and liver damage via PDPN/CLEC-2 in response to APAP stimulation.

In a resting or non-inflammatory state, the expression of PDPN in the liver is minimal. Acute toxic liver injury leads to increased expression of PDPN in resident/

infiltrating liver Kupffer cells.[3] Our data indicate that the C3/C3aR pathway regulates the expression of PDPN on Kupffer cells. Future research should focus on obtaining molecular insights into this regulation. The effect of CLEC-2/PDPN interaction on platelet recruitment and thrombotic inflammation has been confirmed under various inflammatory conditions.[3,47] However, our understanding of the molecular pathways that mediate these effects remains limited.

Previous studies have reported that platelets play an essential role in the physiological and pathological processes related to liver disease.[48] However, platelets may have harmful or beneficial effects in different environments. Their overall impact on liver pathology remains unclear and may vary depending on the disease and its stage.[49] Our data suggests that the interaction between platelet CLEC-2 and PDPN expressed on Kupffer cells leads to platelet recruitment to the liver in AILI. Previous studies have found that activated platelets in the blood sinuses release various growth factors in ALI.[50] It is known that the interaction between platelets and Kupffer cells can regulate the function, differentiation, and cytokine secretion of Kupffer cells.[51,52] Yet, little is known about the molecular mechanisms underlying these effects. This report presents the novel findings regarding the CLEC-2/PDPN pathway that links complement regulation of platelet function with changes in MF cytokine response and, ultimately, how it mediates the recovery of ALI. These findings indicate that platelets may be a therapeutic target for treating liver injury.

In summary, during AILI, the upregulation of C3 expression activates the Kupffer cell membrane receptors C3aR, which induces the expression of Kupffer cell PDPN. Interaction of PDPN with CLEC-2 activates platelets, leading to increased hepatic inflammation and hindering liver repair. Our research has revealed a new role of the C3/C3aR axis in AILI and extensively investigated the mechanism through which C3/C3aR signaling facilitates platelet accumulation and liver damage via PDPN/CLEC-2 in response to APAP stimulation. Considering the challenges in managing patients with severe ALI, this work may hold therapeutic significance, and the interaction between complement regulation and CLEC-2/PDPN may be an exciting topic to explore in human ALF.

AUTHOR CONTRIBUTIONS

Zhanli Xie, Jiang Jiang, Tao Wen, and Xia Bai performed experiments; Zhanli Xie and Jiang Jiang analyzed results and constructed the figures; Zhanli Xie, Fei Yang, Jingjing Han and Zhenni Ma provided intellectual input into the cellular and animal studies; Zhanli Xie, Tao Wen and Xia Bai designed the research and wrote the paper with input from all coauthors, who read, edited, and approved the final manuscript. The order of co-first authors was determined based on the amount of work contributed.

ACKNOWLEDGMENTS

This study was supported by Suzhou People's Livelihood Science and Technology Project (grant no. SKY2022155 and SKJYD2021089), National Natural Science Foundation of China (grant no. 81800128), Suzhou New District Science and Technology Project (grant no. 2020Z002).

DISCLOSURES

The authors have declared that no conflict of interest exists.

DATA AVAILABILITY STATEMENT

Data are available from the corresponding author upon request.

ORCID

Zhanli Xie https://orcid.org/0000-0001-5047-7737
Jiang Jiang https://orcid.org/0009-0006-9463-593X
Fei Yang https://orcid.org/0000-0001-6004-1507
Jingjing Han https://orcid.org/0009-0001-2792-5842
Zhenni Ma https://orcid.org/0009-0009-0182-6457
Tao Wen https://orcid.org/0000-0003-0675-0163
Xia Bai https://orcid.org/0009-0000-5028-453X

REFERENCES

1. Shan Z, Li L, Atkins CL, et al. Chitinase 3-like-1 contributes to acetaminophen-induced liver injury by promoting hepatic platelet recruitment. *Elife*. 2021;10:10.
2. Jaeschke H, Akakpo JY, Umbaugh DS, Ramachandran A. Novel therapeutic approaches against acetaminophen-induced liver injury and acute liver failure. *Toxicol Sci*. 2020;174(2):159-167.
3. Chauhan A, Sheriff L, Hussain MT, et al. The platelet receptor CLEC-2 blocks neutrophil mediated hepatic recovery in acetaminophen induced acute liver failure. *Nat Commun*. 2020;11(1):1939.
4. Rumack BH, Bateman DN. Acetaminophen and acetylcysteine dose and duration: past, present and future. *Clin Toxicol (Phila)*. 2012;50(2):91-98.
5. O'Grady J. Timing and benefit of liver transplantation in acute liver failure. *J Hepatol*. 2014;60(3):663-670.
6. Mossanen JC, Tacke F. Acetaminophen-induced acute liver injury in mice. *Lab Anim*. 2015;49(1 Suppl):30-36.
7. Henderson MW, Sparkenbaugh EM, Wang S, et al. Plasmin-mediated cleavage of high-molecular-weight kininogen contributes to acetaminophen-induced acute liver failure. *Blood*. 2021;138(3):259-272.
8. Laskin DL, Sunil VR, Gardner CR, Laskin JD. Macrophages and tissue injury: agents of defense or destruction? *Annu Rev Pharmacol Toxicol*. 2011;51:267-288.
9. Kusakabe J, Hata K, Miyauchi H, et al. Complement-5 inhibition deters progression of fulminant hepatitis to acute liver failure in murine models. *Cell Mol Gastroenterol Hepatol*. 2021;11(5):1351-1367.

10. Deng M, Gui X, Kim J, et al. LILRB4 signalling in leukaemia cells mediates T cell suppression and tumour infiltration. *Nature*. 2018;562(7728):605-609.
11. Groeneveld D, Cline-Fedewa H, Baker KS, et al. Von Willebrand factor delays liver repair after acetaminophen-induced acute liver injury in mice. *J Hepatol*. 2020;72(1):146-155.
12. Lisman T, Stravitz RT. Rebalanced hemostasis in patients with acute liver failure. *Semin Thromb Hemost*. 2015;41(5):468-473.
13. Lisman T, Luyendyk JP. Platelets as modulators of liver diseases. *Semin Thromb Hemost*. 2018;44(2):114-125.
14. Thorgersen EB, Barratt-Due A, Haugaa H, et al. The role of complement in liver injury, regeneration, and transplantation. *Hepatology*. 2019;70(2):725-736.
15. He S, Atkinson C, Evans Z, et al. A role for complement in the enhanced susceptibility of steatotic livers to ischemia and reperfusion injury. *J Immunol*. 2009;183(7):4764-4772.
16. Li Q, Lu Q, Zhu MQ, et al. Lower level of complement component C3 and C3a in the plasma means poor outcome in the patients with hepatitis B virus related acute-on-chronic liver failure. *BMC Gastroenterol*. 2020;20(1):106.
17. Chen C, Yuan Z, Li W, et al. Complement C3 facilitates stratification of stages of chronic hepatitis B and signifies development of acute-on-chronic liver failure in acute decompensated cirrhosis. *Adv Ther*. 2023;40(3):1171-1186.
18. Casey LC, Fontana RJ, Aday A, et al. Acute liver failure (ALF) in pregnancy: how much is pregnancy related? *Hepatology*. 2020;72(4):1366-1377.
19. Gerard C. Complement C5a in the sepsis syndrome--too much of a good thing? *N Engl J Med*. 2003;348(2):167-169.
20. Xie Z, Shao B, Hoover C, et al. Monocyte upregulation of podoplanin during early sepsis induces complement inhibitor release to protect liver function. JCI. *Insight*. 2020;5(13).
21. Miyakawa K, Joshi N, Sullivan BP, et al. Platelets and protease-activated receptor-4 contribute to acetaminophen-induced liver injury in mice. *Blood*. 2015;126(15):1835-1843.
22. Guerrero Munoz F, Fearon Z. Sex related differences in acetaminophen toxicity in the mouse. *J Toxicol Clin Toxicol*. 1984;22(2):149-156.
23. Sullivan BP, Kassel KM, Jone A, Flick MJ, Luyendyk JP. Fibrin(ogen)-independent role of plasminogen activators in acetaminophen-induced liver injury. *Am J Pathol*. 2012;180(6):2321-2329.
24. Kusakabe J, Hata K, Tamaki I, et al. Complement 5 inhibition ameliorates hepatic ischemia/reperfusion injury in mice, dominantly via the C5a-mediated Cascade. *Transplantation*. 2020;104(10):2065-2077.
25. Li Y, Fu J, Ling Y, et al. Sialylation on O-glycans protects platelets from clearance by liver Kupffer cells. *Proc Natl Acad Sci USA*. 2017;114(31):8360-8365.
26. Singhal R, Ganey PE, Roth RA. Complement activation in acetaminophen-induced liver injury in mice. *J Pharmacol Exp Ther*. 2012;341(2):377-385.
27. Walport MJ. Complement. First of two parts. *N Engl J Med*. 2001;344(14):1058-1066.
28. Holt MP, Cheng L, Ju C. Identification and characterization of infiltrating macrophages in acetaminophen-induced liver injury. *J Leukoc Biol*. 2008;84(6):1410-1421.
29. Grypioti AD, Theocharis SE, Demopoulos CA, Papadopoulou-Daifoti Z, Basayiannis AC, Mykoniatis MG. Effect of platelet-activating factor (PAF) receptor antagonist (BN52021) on acetaminophen-induced acute liver injury and regeneration in rats. *Liver Int*. 2006;26(1):97-105.
30. Mamane Y, Chung Chan C, Lavallee G, et al. The C3a anaphylatoxin receptor is a key mediator of insulin resistance and functions by modulating adipose tissue macrophage infiltration and activation. *Diabetes*. 2009;58(9):2006-2017.
31. Suzuki-Inoue K. Platelets and cancer-associated thrombosis: focusing on the platelet activation receptor CLEC-2 and podoplanin. *Blood*. 2019;134(22):1912-1918.
32. Herzog BH, Fu J, Wilson SJ, et al. Podoplanin maintains high endothelial venule integrity by interacting with platelet CLEC-2. *Nature*. 2013;502(7469):105-109.
33. Ding K, Li X, Ren X, et al. GBP5 promotes liver injury and inflammation by inducing hepatocyte apoptosis. *FASEB J*. 2022;36(1):e22119.
34. Fujii M, Honma M, Takahashi H, Ishida-Yamamoto A, Iizuka H. Intercellular contact augments epidermal growth factor receptor (EGFR) and signal transducer and activator of transcription 3 (STAT3)-activation which increases podoplanin-expression in order to promote squamous cell carcinoma motility. *Cell Signal*. 2013;25(4):760-765.
35. Das M, Sabio G, Jiang F, et al. Induction of hepatitis by JNK-mediated expression of TNF-alpha. *Cell*. 2009;136(2):249-260.
36. Ilyas G, Zhao E, Liu K, et al. Macrophage autophagy limits acute toxic liver injury in mice through down regulation of interleukin-1beta. *J Hepatol*. 2016;64(1):118-127.
37. Hu JJ, Lee MJ, Vapiwala M, Reuhl K, Thomas PE, Yang CS. Sex-related differences in mouse renal metabolism and toxicity of acetaminophen. *Toxicol Appl Pharmacol*. 1993;122(1):16-26.
38. Tujios S, Fontana RJ. Mechanisms of drug-induced liver injury: from bedside to bench. *Nat Rev Gastroenterol Hepatol*. 2011;8(4):202-211.
39. Miao J, Yao S, Sun H, et al. Protective effect of water-soluble Acacetin prodrug on APAP-induced acute liver injury is associated with upregulation of PPARgamma and alleviation of ER stress. *Int J Mol Sci*. 2023;24(14),11320.
40. Guo Z, Chen J, Zeng Y, et al. Complement inhibition alleviates Cholestatic liver injury through mediating macrophage infiltration and function in mice. *Front Immunol*. 2021;12:785287.
41. Keshari RS, Silasi R, Popescu NI, et al. Inhibition of complement C5 protects against organ failure and reduces mortality in a baboon model of Escherichia coli sepsis. *Proc Natl Acad Sci USA*. 2017;114(31):E6390-E6399.
42. Zhang LY, Pan J, Mamtilahun M, et al. Microglia exacerbate white matter injury via complement C3/C3aR pathway after hypoperfusion. *Theranostics*. 2020;10(1):74-90.
43. Krenkel O, Tacke F. Liver macrophages in tissue homeostasis and disease. *Nat Rev Immunol*. 2017;17(5):306-321.
44. Li Z, Weinman SA. Regulation of hepatic inflammation via macrophage cell death. *Semin Liver Dis*. 2018;38(4):340-350.
45. Duffield JS, Forbes SJ, Constandinou CM, et al. Selective depletion of macrophages reveals distinct, opposing roles during liver injury and repair. *J Clin Invest*. 2005;115(1):56-65.
46. Ju C, Reilly TP, Bourdi M, et al. Protective role of Kupffer cells in acetaminophen-induced hepatic injury in mice. *Chem Res Toxicol*. 2002;15(12):1504-1513.
47. Hitchcock JR, Cook CN, Bobat S, et al. Inflammation drives thrombosis after salmonella infection via CLEC-2 on platelets. *J Clin Invest*. 2015;125(12):4429-4446.

48. Nicolai L, Schiefelbein K, Lipsky S, et al. Author correction: vascular surveillance by haptotactic blood platelets in inflammation and infection. *Nat Commun*. 2022;13(1):4645.
49. Rayes J, Lax S, Wichaiyo S, et al. The podoplanin-CLEC-2 axis inhibits inflammation in sepsis. *Nat Commun*. 2017;8(1):2239.
50. Meyer J, Lejmi E, Fontana P, Morel P, Gonelle-Gispert C, Bühler L. A focus on the role of platelets in liver regeneration: do platelet-endothelial cell interactions initiate the regenerative process? *J Hepatol*. 2015;63(5):1263-1271.
51. Hottz ED, Medeiros-de-Moraes IM, Vieira-de-Abreu A, et al. Platelet activation and apoptosis modulate monocyte inflammatory responses in dengue. *J Immunol*. 2014;193(4):1864-1872.
52. Mantovani A, Garlanda C. Platelet-macrophage partnership in innate immunity and inflammation. *Nat Immunol*. 2013;14(8):768-770.

SUPPORTING INFORMATION

Additional supporting information can be found online in the Supporting Information section at the end of this article.

How to cite this article: Xie Z, Jiang J, Yang F, et al. The C3/C3aR pathway exacerbates acetaminophen-induced mouse liver injury via upregulating podoplanin on the macrophage. *The FASEB Journal*. 2025;39:e70272. doi:10.1096/fj.202402278RR